ELSEVIER

Polymer 43 (2002) 4887–4894

polymer

www.elsevier.com/locate/polymer

Effect of molecular weight on the electrorheological behavior of side-chain liquid crystal polymers in nematic solvents

Yen-Ching Chiang[a], Alex M. Jamieson[a,*], Yiqiang Zhao[a], Andrea M. Kasko[b], Coleen Pugh[b]

[a]*Department of Macromolecular Science and Engineering, Case Western Reserve University, 2100 Adelbert Road, Cleveland, OH 44106-7202, USA*
[b]*Department of Polymer Science, Maurice Morton Institute of Polymer Science, The University of Akron, Akron, OH, USA*

Received 28 February 2002; received in revised form 13 May 2002; accepted 15 May 2002

Abstract

We investigate the change in the electrorheological (ER) properties of a nematic solvent on dissolution of an end-on polyacrylate side-chain liquid crystal polymer (SCLCP) with an 11-methylene spacer. We observe a weak enhancement of the ER response, $\Delta\eta = \delta\eta_{on} - \delta\eta_{off}$, where $\delta\eta_{on}$ is the viscosity increment on dissolving polymer in the presence of a strong electric field, applied transverse to the flow, and $\delta\eta_{off}$ is the corresponding increment in the absence of the field. Equating η_{on} and η_{off}, respectively, to the Miesowicz viscosities η_c and η_b, and using the theoretical prediction that $\delta\eta_c/\delta\eta_b = R_{\parallel}^4/R_{\perp}^4$, where $R_{\parallel}$ and $R_{\perp}$ are the rms end-to-end distances of the chain parallel and perpendicular to the director, this indicates that the chain conformation of the SCLCP is weakly prolate. The molecular weight dependence of the conformational relaxation time, τ_r, also extracted via the hydrodynamic theory, is identical to that deduced from the GPC hydrodynamic volume in tetrahydrofuran as solvent. The hydrodynamic volume in the nematic state is larger, however, and increases with decrease in temperature. An earlier study of a polysiloxane SCLCP observed similar behavior, but with a smaller molecular weight dependence of τ_r. The difference is ascribed to dissimilar chain conformations of the two SCLCPs.

Keywords: Electrorheology; Side-chain liquid crystal polymer; Chain conformation

1. Introduction

Low molar mass nematic materials with positive dielectric anisotropy, $\Delta\varepsilon > 0$, exhibit a small electrorheological (ER) effect [1,2] since, when a field is applied in the direction of the shear gradient, the electric torque aligns the director perpendicular to the flow, whereas, with the field off, the director is rotated by the viscous torque toward the flow direction. Thus, the viscosity with the field on, η_{on}, is greater than that, η_{off}, with the field off. A similar phenomenon is observed when such a field is applied to tumbling nematics, i.e. the field suppresses the tumbling process [1,2]. The ER properties of liquid crystalline polymer solutions have been studied by several groups [3–7]. Yang and Shine demonstrated that lyotropic solutions of the stiff-chain polymer, poly(*n*-hexyl isocyanate) show a large ER effect in the presence of both DC and AC fields [3,4]. These authors also reported [3,4] that the director tumbling behavior which occurs in such solutions is suppressed when the applied field is sufficiently strong, and, at low shear strain and low shear rate, it is possible to measure the Miesowicz viscosity η_c, where the director is pinned in the direction of the shear gradient, perpendicular to the flow.

Previous studies [5,6] from our laboratory showed that dissolution of a main-chain liquid crystal polymer (MCLCP) in a low molar mass nematic solvent with $\Delta\varepsilon > 0$ strongly increases the ER response, defined as the difference between the value of the viscosity measured in the presence, η_{on}, and absence, η_{off}, of the applied field, whereas a side-on side-chain liquid crystal polymer (SCLCP) moderately increases the response [6], and an end-on SCLCP weakly affects the response [6,7]. This can be explained by assuming that the MCLCP has a highly prolate conformation, with the chain stretched along the nematic director, and that the field will align the long axis perpendicular to the flow, leading to a large increase in η_{on}. When the field is switched off, the long axis rotates with the nematic director and aligns near the flow direction, resulting in a relatively weak viscosity increment, $\delta\eta_{off}$. A side-on SCLCP, where the mesogen is attached parallel to the

* Corresponding author. Tel.: +1-216-368-4172; fax: +1-216-368-4202.
E-mail address: amj@po.cwru.edu (A.M. Jamieson).

0032-3861/01/$ - see front matter
PII: S0032-3861(02)00328-2

backbone, also has a prolate conformation, but not so asymmetric as a MCLCP, and an end-on SCLCP, with mesogen perpendicular to the backbone, has a quasi-spherical conformation. Such conformational differences are qualitatively consistent with theoretical analysis of the effect of molecular architecture on liquid crystal polymer (LCP) conformation [8].

We measured η_{on} and η_{off}, using a controlled-stress rheometer with cone and plate geometry [5–7], which ensures uniform shear deformation of the fluid throughout the radial direction. However, the magnitude of the applied field varies radially. As described by Yang and Shine [3], in the presence of a sufficiently strong field, at low shear rate, the director is pinned perpendicular to the shear flow, and η_{on} corresponds to the Miesowicz viscosity, η_c. When the electric field is switched off, for flow-aligning nematics, the director rotates near the flow direction and η_{off} is close to, though slightly larger than, the Miesowicz viscosity η_b, which corresponds to the director fixed parallel to the flow direction. For the MCLCP, we found that the viscosity increment, $\delta\eta_{on}$ was a strong function of the LCP molecular weight, and that $\delta\eta_{off}$ had a somewhat weaker dependence on molecular weight [5,6]. In contrast, for an end-on SCLCP, with a polysiloxane backbone, we found that $\delta\eta_{on}$ was independent of the LCP molecular weight, and that $\delta\eta_{off}$ had a modest molecular weight dependence [7].

These results were quantitatively interpreted [5–7] in terms of a hydrodynamic theory by Brochard [9]. This theory generates expressions for the increments in η_c and η_b in terms of the rms end-to-end distances of the chain, $R_\parallel$ and $R_\perp$, respectively, parallel and perpendicular to the director:

$$\delta\eta_b = \left(\frac{ckT}{N}\right)\tau_r\left(\frac{R_\perp^2}{R_\parallel^2}\right) \tag{1}$$

$$\delta\eta_c = \left(\frac{ckT}{N}\right)\tau_r\left(\frac{R_\parallel^2}{R_\perp^2}\right) \tag{2}$$

Hence

$$\left(\frac{\delta\eta_c}{\delta\eta_b}\right) = \left(\frac{R_\parallel}{R_\perp}\right)^4 \tag{3}$$

Here, c is polymer concentration (monomers/ml), N is the degrees of polymerization of the polymer, T is absolute temperature, k is the Boltzmann's constant, and τ_r is the polymer conformational relaxation time, which is related to the anisotropic frictional coefficients for translational motion of the chain, $\lambda_\parallel$ and $\lambda_\perp$,

$$\frac{1}{\tau_r} = \frac{kT}{\lambda_\parallel R_\parallel^2} + \frac{kT}{\lambda_\perp R_\perp^2} \tag{4}$$

Parenthetically, we remark that, in our previous work [10], we were able to theoretically correlate experimental data on the Miesowicz viscosity increments, $\delta\eta_b$ and $\delta\eta_c$, with that on the Leslie viscosity increments, $\delta\alpha_2$ and $\delta\alpha_3$, where the nematic director is free to rotate. To accomplish this, it is necessary to introduce into the Brochard model a new term, reflecting a mechanical coupling between director rotation and chain conformation [10].

For MCLCPs, the observed strong ER response is consistent with Eq. (3) [5], since the LCP chain conformation is highly prolate [11], $R_\parallel \gg R_\perp$. Likewise, for the polysiloxane end-on SCLCP, the observed ER effect agrees with Eq. (3), since the conformation is quasi-spherical [11,12], $R_\parallel \approx R_\perp$, and may be slightly prolate or oblate, depending on the molecular weight and spacer length [7,9]. An interesting feature of the latter results is that the intrinsic viscosity with the field on, $[\eta_{on}]$, and the associated apparent hydrodynamic volume, $V_{h,on}$, are each smaller than with the field off, $[\eta_{off}]$ and $V_{h,off}$. In fact, this is easily shown to be consistent with the Brochard theory. From Eqs. (1) and (2), for a particle which has a spherically symmetric conformation, i.e. $R_\parallel = R_\perp = R/\sqrt{3}$, where R is the rotationally averaged rms end-to-end distance, it follows immediately that

$$\delta\eta_b = \delta\eta_c = \left(\frac{cR^2}{3N}\right)\frac{\lambda_\parallel\lambda_\perp}{\lambda_\parallel + \lambda_\perp} \tag{5}$$

Thus, it is clear that the origin of any difference between $[\eta_b]$ and $[\eta_c]$ must arise in the anisotropic hydrodynamics in the nematic state, i.e. because $\lambda_\parallel \neq \lambda_\perp$. As discussed by Wang [13], a detailed accounting of the hydrodynamics of a flexible polymer chain in a nematic fluid is complex. Here, we assume simply that the particle behaves as an impermeable sphere of radius R_h, and that the frictional anisotropy of motion parallel and perpendicular to the director is determined by the fact that the controlling medium viscosities are, respectively, the solvent Miesowicz viscosities η_b^0 and η_c^0. Hence we can write expressions of the Stokes form: $\lambda_\parallel = 6\pi\eta_b^0 R_h$ and $\lambda_\perp = 6\pi\eta_c^0 R_h$, and obtain:

$$\delta\eta_b = \delta\eta_c = \frac{\pi cR^2 R_h}{N}\left(\frac{2\eta_b^0\eta_c^0}{\eta_b^0 + \eta_c^0}\right) \tag{6}$$

Eq. (6) indicates that the effective solvent viscosity for the conformational relaxation time of a spherically symmetric, impermeable particle in the nematic state is $2\eta_b^0\eta_c^0/(\eta_b^0 + \eta_c^0)$. Since $\eta_b^0 < \eta_c^0$, we have $\delta\eta_b/\eta_b^0 > \delta\eta_c/\eta_c^0$ and therefore $[\eta_c] > [\eta_b]$.

The question arises whether these novel behaviors are influenced by the structure of the polymer backbone? In the present paper, we explore this issue for a different end-on SCLCP, poly[11-(4′-cyanophenyl-4″-phenoxy)undecyl acrylate] [14], having a polyacrylate backbone and cyanobiphenyl mesogen, attached via an undecyl spacer, and dissolved in a commercial nematic mixture, E48. We find that, while the rheology of dilute nematic solutions of this SCLCP has many similarities to the earlier study of a polysiloxane end-on SCLCP, the molecular weight dependence is distinctly different, indicative of dissimilar chain conformations of the two polymers.

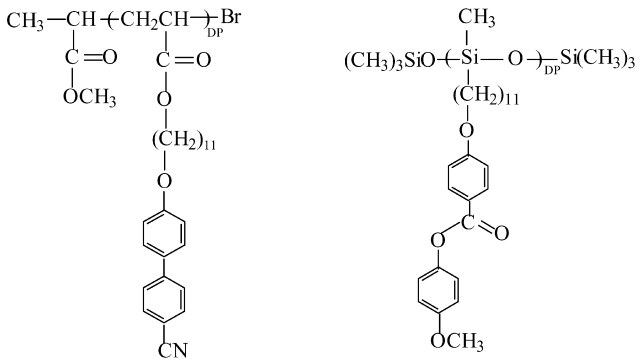

(a) Polyacrylate SCLCP (b) Polysiloxane SCLCP

Fig. 1. Molecular structures of end-on side-chain liquid crystalline polymers (end-on SCLCP) with same spacer length ($n = 11$) : (a) end-on polyacrylate SCLCP, poly[11-(4′-cyanophenyl-4″-phenoxy)undecyl acrylate]; (b) end-on polysiloxane SCLCP.

2. Experimental

2.1. Materials

The end-on SCLCP, poly[11-(4′-cyanophenyl-4″-phenoxy)undecyl acrylate], whose structure is shown in Fig. 1(a), was studied in this work. Samples with different molecular weights were contributed by Prof. C. Pugh of the University of Akron. Details of the synthesis and characterization of these polymers are given elsewhere [14]. The apparent molecular weights [14] (measured by GPC in tetrahydrofuran (THF) as solvent, relative to polystyrene standards), as well as the true molecular weights [15] (measured by GPC in THF as solvent with a light scattering detector), are listed in Table 1. We compare the present results with literature data on a polysiloxane end-on SCLCP, also having an undecyl spacer, whose structure is shown in Fig. 1(b), and whose molecular weight data are listed for convenience in Table 2. All LCP specimens were used without further purification. The nematic solvent used in this study was a commercial mixture of cyanobiphenyls, referred to as E48, which has an extended nematic temperature range ($T_{NI} = 85$ °C), and was obtained from BDH Ltd. The solvent used in our earlier study was 4′-(pentyloxy)-4-cyanobiphenyl (5OCB, $T_{NI} = 67$ °C).

2.2. Sample preparation and measurements

A specified weight of LCP was dissolved in the nematic solvent at a temperature above its clearing temperature. Equilibration was continued (typically requiring at least 24 h) until complete dissolution to form an isotropic solution. Using a micro-pipette, nematic samples were placed on the plate of the Carri–Med controlled stress rheometer with cone-and-plate geometry ($D = 2$ cm, angle = 0.5°), pre-equilibrated at a selected temperature for at least 10 min. The sample quantity was approximately

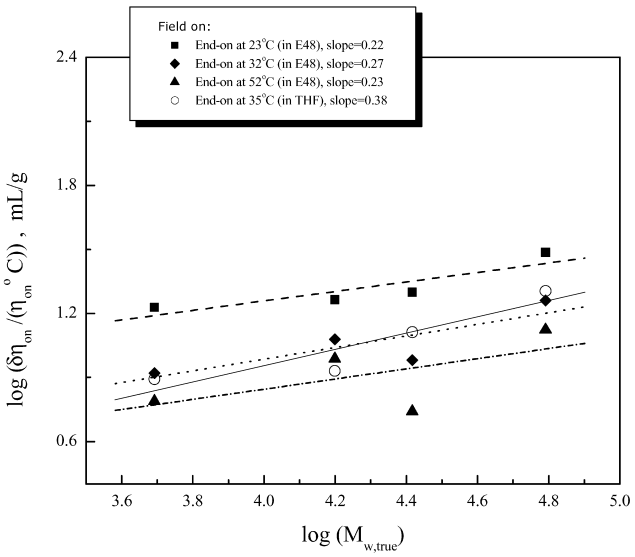

(a)

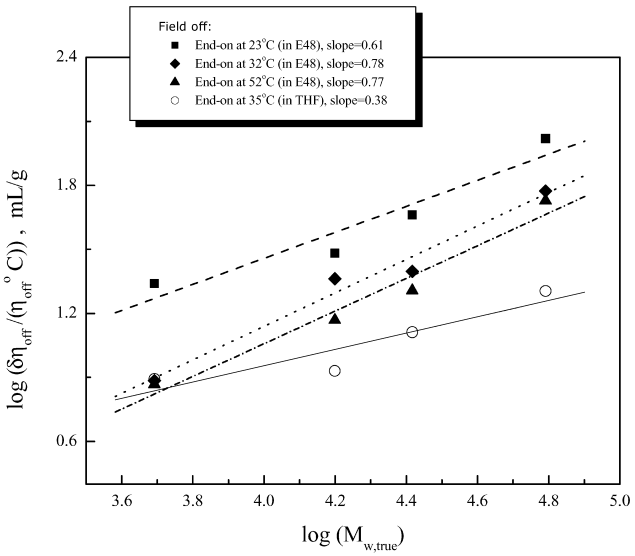

(b)

Fig. 2. Molecular weight dependence of the reduced specific viscosity increments ($\delta\eta_{on}/\eta^0_{on}c$ and $\delta\eta_{off}/\eta^0_{off}c$) for side-chain liquid crystalline polyacrylates in E48 at various temperatures. (a) Field on; (b) field off. Also shown in each panel are the values in THF at 35 °C, computed from the GPC hydrodynamic volumes as $\delta\eta/\eta^0 c = 2.5\, N_A V_h/M_w$.

35 μl. Then the shear sweep method [5–7] was applied to measure the viscosity response in the low-shear limit, with or without a strong electric field ($E = 2.2$ kV/mm, computed as the mean value integrated from the cone tip to the rim). As shown in earlier work [5–7], this field is high enough to assure complete alignment in the low-shear limit. The detailed experimental methods are given elsewhere [5–7]. Particular care was taken to ensure that the solution totally filled the gap between the cone and plate, and that no air bubbles were present in the sample.

Table 1
Molecular weights of side-chain liquid crystalline polyacrylates

GPC_{PSt}[a]			GPC-LS[b]			
M_w ($\times 10^3$ g/mol)	M_n ($\times 10^3$ g/mol)	PDI	DP_n[c]	$M_{w,true}$ ($\times 10^3$ g/mol)	$M_{n,true}$ ($\times 10^3$ g/mol)	PDI
5.86	5.05	1.16	9	4.92	4.01	1.23
12.1	10.0	1.21	28	15.8	12.0	1.32
20.6	15.4	1.34	52	26.1	21.9	1.19
43.8	29.4	1.49	100[d]	61.8[d]	42.2[d]	1.46

[a] Apparent molecular weights measured by GPC in THF as solvent at 35 °C, relative to polystyrene standards.
[b] True molecular weights measured by GPC in THF as solvent with a light scattering detector.
[c] DP_n, true number average degree of polymerization of backbones.
[d] Calculated value based on the fitted relations [14] $(M_{w,true} \times 10^{-3}) = 1.512(M_{w,GPCPSt} \times 10^{-3}) - 2.222$ and $(M_{n,true} \times 10^{-3}) = 1.461(M_{n,GPCPSt} \times 10^{-3}) - 2.198$.

3. Results and discussions

3.1. Viscosity measurements

The shear viscosities with field on and field off, $\delta\eta_{on}$ and $\delta\eta_{off}$, respectively, were measured for a 3 wt% solution of the polyacrylate SCLCP dissolved in the mixed nematic solvent E48, and also for the solvent alone, at several temperatures in the nematic state. This concentration is in the dilute solution range, where linear dependence of the viscosity increment on SCLCP concentration is observed in accord with Eqs. (1) and (2). The results are tabulated in Table 3. The corresponding reduced specific viscosity increments, $\delta\eta_{on}/\eta^0_{on}c$ and $\delta\eta_{off}/\eta^0_{off}c$, are plotted logarithmically against true molecular weight in Fig. 2. Each quantity exhibits significant molecular weight dependence, approximately as $\delta\eta_{on}/\eta^0_{on}c \sim M_w^{0.2}$ and $\delta\eta_{off}/\eta^0_{off}c \sim M_w^{0.7}$, only slightly influenced by temperature. Also plotted in Fig. 2 are the estimated values $(\delta\eta/\eta^0 c \approx 2.5N_A V_h/M_w)$ of the polymer in THF, calculated from the GPC hydrodynamic volumes, V_h, and the true weight-average molecular weights of the SCLCP, M_w. To obtain V_h, the intrinsic viscosity $[\eta]_{PS/THF}$ of a polystyrene with the equivalent hydrodynamic volume was first computed from the apparent GPC weight-average molecular weight of the SCLCP, M_{PS}, calibrated against polystyrene, using the Mark–Houwink relations for polystyrene in THF at 25 °C [16]:

$$[\eta]_{PS/THF}(25\,^\circ\mathrm{C}) = 11.64 \times 10^{-3} M_{PS}^{0.73} \quad (7)$$

The hydrodynamic volume, V_h, was then obtained directly via the Einstein equation:

$$[\eta]_{PS/THF} = 2.5N_A V_h/M_{PS} \quad (8)$$

For the polyacrylate SCLCP dissolved in the GPC solvent THF, the corresponding viscosity scaling exponent $(\delta\eta_{iso}/\eta^0_{iso}c \sim M_w^{0.38})$ is intermediate between those for $\delta\eta_{on}$ and $\delta\eta_{off}$, and the values of $\delta\eta_{iso}/\eta^0_{iso}c$ are numerically comparable to $\delta\eta_{on}/\eta^0_{on}c$ and smaller than $\delta\eta_{off}/\eta^0_{off}c$.

These results contrast with our previous study [7] of a polysiloxane SCLCP also having an undecyl spacer, dissolved in nematic 5OCB at 62 °C, where we found $\delta\eta_{on} \sim M_w^{0.03}$ and $\delta\eta_{off} \sim M_w^{0.27}$, and $\delta\eta_{iso}/\eta^0_{iso}c \sim M_w^{-0.17}$ in the GPC solvent THF (as shown in Table 4 and Fig. 3).

Table 2
Molecular weights of side-chain liquid crystalline polysiloxanes

GPC_{PSt}[a]			True MW[b]		
	M_n ($\times 10^3$ g/mol)	PDI	DP_n[c]	$M_{w,true}$ ($\times 10^3$ g/mol)	$M_{n,true}$ ($\times 10^3$ g/mol)
11.5	9.8	1.17	45	24.2	20.7
14.0	9.7	1.44	72	47.5	33.0
22.1	11.7	1.89	127	109.8	58.1
33.3	13.1	2.54	198	229.7	90.5

[a] Apparent molecular weights measured by GPC in THF as solvent at 25 °C, relative to polystyrene standards.
[b] True molecular weights calculated from degree of polymerization of polysiloxane LCP.
[c] DP_n, true number average degree of polymerization of backbones.

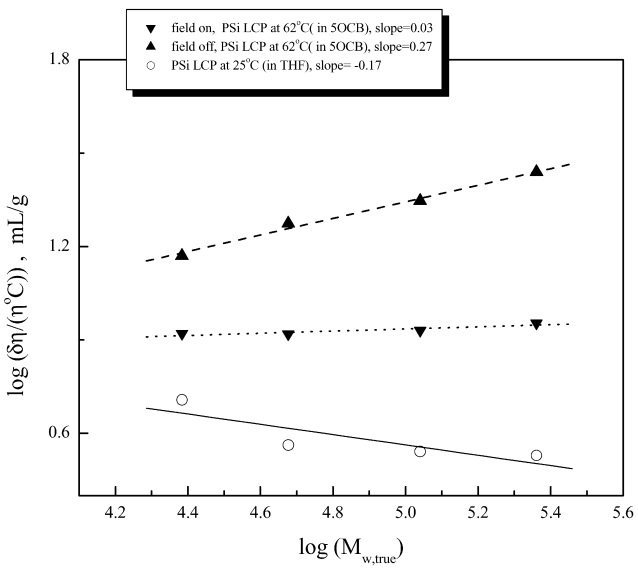

Fig. 3. Molecular weight dependence of the viscosity increments $(\delta\eta_{on}/\eta^0_{on}c$ and $\delta\eta_{off}/\eta^0_{off}c)$ for side-chain liquid crystalline polysiloxanes in 5OCB at 62 °C. (a) Field on; (b) field off. Also shown are the corresponding values in THF at 25 °C computed from the GPC hydrodynamic volumes as $\delta\eta/\eta^0 c = 2.5N_A V_h/M_w$.

Table 3
Hydrodynamic parameters of side-chain liquid crystalline polyacrylates in E48 from ER measurements

DP_n	$\delta\eta_{on}/c$ (P ml/g)			$\delta\eta_{off}/c$ (P ml/g)			$R_\parallel/R_\perp$			τ_r (μS)[a]			$\delta\eta_{iso}/c$[b] (P ml/g)	τ_r (μS)[b] in THF
	23 °C	32 °C	52 °C	23 °C	32 °C	52 °C	23 °C	32 °C	52 °C	23 °C	32 °C	52 °C	35 °C	35 °C
9	41.97	14.15	4.56	7.43	1.92	0.96	1.54	1.63	1.49	3.54	1.04	0.37	0.0323	0.04
28	45.56	20.38	7.19	10.31	5.76	1.92	1.44	1.37	1.38	14.2	6.78	2.24	0.0353	0.14
52	49.40	16.31	4.08	15.59	6.24	2.64	1.33	1.27	1.1	29.76	10.43	3.62	0.0536	0.34
100	76.02	30.94	9.83	35.49	14.87	6.95	1.21	1.2	1.09	130.2	52.45	19.01	0.0835	1.25

[a] τ_r, conformational relaxation time.
[b] THF as a solvent at 35 °C.

Bearing in mind that changes in nematic solvent type, temperature and sample polydispersity will have an influence on the solution viscosity, the different exponents suggest that the polyacrylate SCLCP may adopt a less compact chain conformation to that of the polysiloxane SCLCP.

3.2. Chain anisotropy and relaxation time

Applying Eqs. (1)–(3), we extract values of the ratio $R_\parallel/R_\perp$ and τ_r, which are listed in Table 3. The corresponding analysis, performed previously [7] for the polysiloxane SCLCP, is presented in Table 4. In each case, the Brochard model provides a quantitative self-consistent interpretation of the observed values of $\delta\eta_{on}$ and $\delta\eta_{off}$. Table 3 indicates that the chain conformation is prolate ($R_\parallel/R_\perp > 1$), and that there is a systematic decrease in the ratio $R_\parallel/R_\perp$ with increasing molecular weight of the polyacrylate SCLCP, and also, at fixed molecular weight, a decreasing trend in $R_\parallel/R_\perp$ with increase in temperature. On the other hand, the conformational relaxation time τ_r increases strongly with increase in molecular weight and decrease in temperature. Moreover, as shown in Fig. 4, the molecular weight dependence, $\tau_r \sim M_w^{1.5}$ is similar to that ($\tau_r \sim M_w^{1.4}$) of the corresponding relaxation time in THF at 35 °C, computed from the GPC hydrodynamic volumes, V_h, as $\tau_r = 15\eta_s V_h/kT$.

The equivalent analysis of the earlier data on the polysiloxane SCLCP indicates a similar behavior (Table 4). The polysiloxane chain has a distinctly prolate conformation at low molecular weight ($R_\parallel/R_\perp > 1$), which again becomes more spherical as the molecular weight increases. Likewise, as shown in Fig. 5, τ_r has a molecular weight dependence essentially identical to that deduced for the polysiloxane SCLCP in THF, but with a significantly smaller molecular weight exponent ($\tau_r \sim M_w^{0.8}$) compared to the polyacrylate SCLCP.

The above observations conflict with the theoretical prediction that the conformation of an end-on SCLCP will be oblate, based on analysis of the coupling between the backbone orientation and the nematic field [8]. However, the existence of prolate conformations for polyacrylate end-on SCLCPs under certain conditions has been confirmed by scattering methods in the bulk state [11]. These anomalies

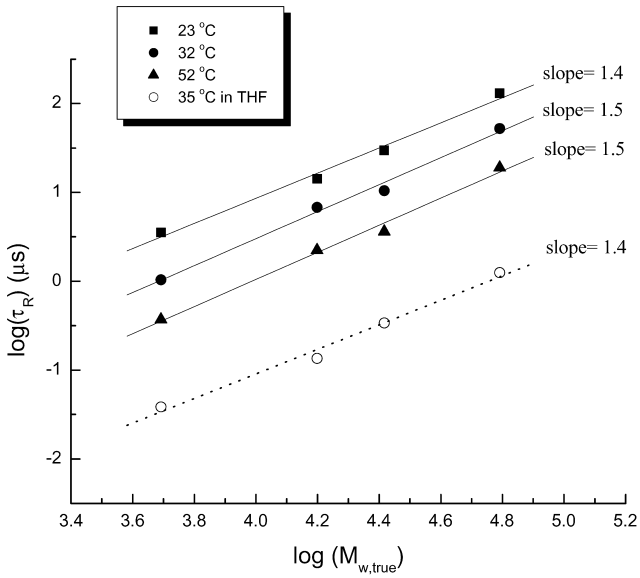

Fig. 4. Log–log plot of molecular weight dependence of conformational relaxation times τ_r, for side-chain liquid crystalline polyacrylates in E48 at various temperatures compared to values in THF at 35 °C calculated from GPC hydrodynamic volumes as $\tau_r = 15\eta_s V_h/kT$.

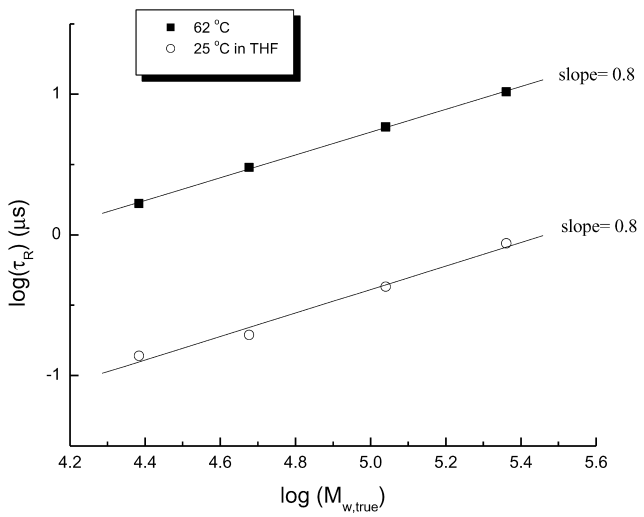

Fig. 5. Log–log plot of molecular weight dependence of conformational relaxation times τ_r, for side-chain liquid crystalline polysiloxanes in 5OCB at 62 °C compared to values in THF at 25 °C calculated from GPC hydrodynamic volumes as $\tau_r = 15\eta_s V_h/kT$.

Table 4
Hydrodynamic parameters of side-chain liquid crystalline polysiloxanes in 5OCB ($n = 11$, at 62 °C)

DP_n	$\delta\eta_{on}/c$ (P ml/g)	$\delta\eta_{off}/c$ (P ml/g)	$R_{\parallel}/R_{\perp}$	τ_r (μS)[a]	$\delta\eta_{iso}/c$ (P ml/g)[b]	τ_r (μS)[b] in THF
45	3.159	1.626	1.18	1.67	0.0235	0.14
72	3.146	2.069	1.11	3.01	0.0169	0.19
127	3.234	2.444	1.07	5.85	0.0161	0.43
198	3.414	3.025	1.03	10.4	0.0156	0.87

[a] τ_r, conformational relaxation time.
[b] THF as a solvent at 25 °C.

have been attributed to a dominant contribution of excluded volume interactions of the spacer [11]. Such an effect is likely for the present polymers with relatively long undecyl spacers. Indeed, in our previous studies of the polysiloxane SCLCP, oblate conformations were indicated by the ER data for polymers with the $n = 3$ spacer [7]. The above observations further indicate dissimilar conformations for the two SCLCPs, which may be ascribed to the difference in rigidity of the backbone. Specifically, the polysiloxane SCLCP, which has a more flexible backbone, forms a compact, globular conformation ($\tau_r \sim V_h \sim M_w^{0.8}$), whereas the more rigid polyacrylate SCLCP has an extended conformation ($\tau_r \sim V_h \sim M_w^{1.5}$). Note that, although the latter scaling relation is similar to that of a random coil, i.e. $\tau_r \sim M^{1.5-1.8}$, this does not imply that the chain is Gaussian, because of the comb-like architecture of the SCLCP, and the fact that the overwhelming majority of the SCLCP mass resides in the side-chains.

Next, we point out that, when corrected for the differences in temperature and viscosity, the effective hydrodynamic radii in the nematic state, $R_{h,nem}$, are typically larger than those, $R_{h,iso}$, computed from the hydrodynamic volumes measured by GPC, as shown in Fig. 6. Here we note that, following Eq. (6)

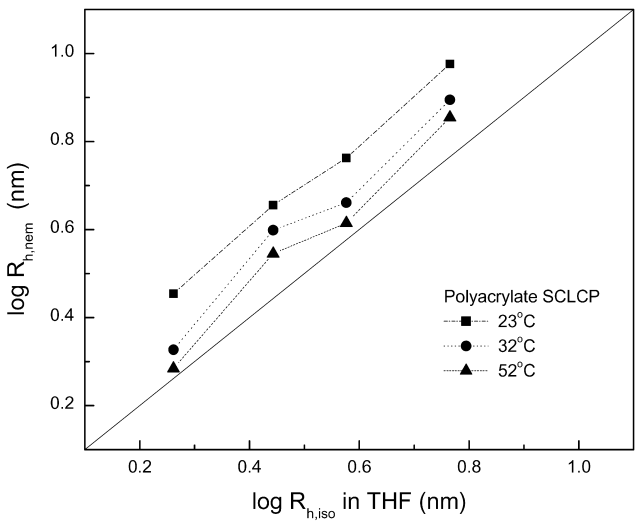

Fig. 6. Log–log plot of $R_{h,nem}$, the effective hydrodynamic radii in the nematic state for side-chain liquid crystalline polyacrylates in E48 at various temperatures, versus $R_{h,iso}$, isotropic hydrodynamic radii in THF at 35 °C for polyacrylates SCLCP; straight line indicates $R_{h,nem} = R_{h,iso}$.

$$R_{h,nem} = \left[\frac{3}{4\pi}\left(\frac{\tau_r kT(\eta_b^0 + \eta_c^0)}{5\eta_b^0\eta_c^0}\right)\right]^{1/3} \quad (9)$$

As evident in Fig. 6, the experimental data fall approximately 5–65% above the straight line which corresponds to $R_{h,nem} = R_{h,iso}$. Recognizing that Eq. (9) assumes spherical particles, and that this comparison does not take into account the significant polydispersity of the two SCLCPs, this may be viewed as reasonable agreement.

The 5–65% discrepancy between $R_{h,nem}$ and $R_{h,iso}$ could be a reflection of a difference in hydrodynamics of the polymer or due to neglect of the conformational asymmetry in making the comparison? The former possibility seems inadmissible, since the similarity in the molecular weight dependence of τ_r in the nematic state versus THF suggests similar hydrodynamics. Therefore, we assess the degree to which neglect of the conformational asymmetry in the ER data for the nematic solution influences the comparison against the GPC hydrodynamic volumes. Such an analysis can be performed for the polyacrylate SCLCP, which has a relatively narrow molecular weight distribution (Table 1).

To accomplish this, we need to incorporate expressions for the frictional coefficients $\lambda_{\parallel}$ and $\lambda_{\perp}$ into the Brochard hydrodynamic model. Again, we make the simplifying assumption that we can adopt expressions for steady translation of an impermeable ellipsoid in a viscous liquid [17]. To evaluate $\lambda_{\parallel}$, we use an expression [17] for fluid motion parallel to the axis of symmetry of a prolate ellipsoid of aspect ratio $\phi = a/c$, where a and c are long and short hydrodynamic semi-axis length, respectively, again assuming the medium viscosity is η_b^0

$$\lambda_{\parallel} = 6\pi\eta_b^0 R_{h\parallel} = 6\pi\eta_b^0\kappa_{\parallel}c \quad (10)$$

where

$$\kappa_{\parallel}^{-1} = \frac{3}{8}\left[-\frac{2\phi}{\phi^2-1} + \frac{2\phi^2-1}{(\phi^2-1)^{3/2}}\ln\left(\frac{\phi+\sqrt{\phi^2-1}}{\phi-\sqrt{\phi^2-1}}\right)\right] \quad (11)$$

When fluid motion is perpendicular to the axis of symmetry, and assuming the effective medium viscosity is η_c^0, the corresponding frictional coefficient is [17]

$$\lambda_{\perp} = 6\pi\eta_c^0 R_{h\perp} = 6\pi\eta_c^0\kappa_{\perp}c \quad (12)$$

Table 5
Molecular hydrodynamic dimensions of polyacrylates SCLCP at 52 °C obtained by fitting ratio x

DP_n	$R_{\parallel}$ (nm)	$R_{\perp}$ (nm)	R_{nem} (nm)[a]	R_{iso} (nm)[b]	a (∥, nm)[c]	c (⊥ , nm)[c]	$R_{h\parallel}$ (nm)	$R_{h\perp}$ (nm)	$R_{h,iso}$ (THF) = $R_{h,nem}$[d] (nm)	Fitting ratio x
9	2.3	1.5	3.2	3.0	2.4	1.6	1.8	1.9	1.8	1.0
28	4.5	3.2	6.4	6.3	3.4	2.5	2.7	2.9	2.8	1.3
52	4.6	4.2	7.6	7.5	4.0	3.7	3.7	3.8	3.8	1.2
100	8.5	7.8	14.0	14.0	6.2	5.7	5.8	5.9	5.8	1.4

[a] $(R_{nem})^2 = R_{\parallel}^2 + 2R_{\perp}^2$.
[b] $x = R_{\perp}/c = R_{\parallel}/a = R_{iso}/\sqrt{3}R_{h,iso}$.
[c] a is long semi-axis length and c is short semi-axis length, ∥ and ⊥ represent the direction parallel and perpendicular to the director $\vec{n}$.
[d] $(R_{h,nem})^3 = ac^2$, and $R_{h,iso}$ for THF at 35 °C.

where

$$\kappa_{\perp}^{-1} = \frac{3}{8}\left[\frac{\phi}{\phi^2-1} + \frac{2\phi^2-3}{(\phi^2-1)^{3/2}}\ln\left(\phi+\sqrt{\phi^2-1}\right)\right] \quad (13)$$

We introduce a single fitting parameter x for the relationship between rms end-to-end distance and hydrodynamic semi-axis length: $x = R_{\parallel}/a = R_{\perp}/c$. This amounts to a further assumption that the coil permeability parallel and perpendicular to the director is the same. Combining Eqs. (10)–(13) with the Brochard model (Eq. (4)), we obtain

$$c^3 = \frac{\tau_r kT\left[\eta_c^0\kappa_{\perp} + \eta_b^0\kappa_{\parallel}\left(\frac{R_{\parallel}}{R_{\perp}}\right)^2\right]}{6x^2\pi\eta_c^0\eta_b^0\kappa_{\parallel}\kappa_{\perp}\left(\frac{R_{\parallel}}{R_{\perp}}\right)^2} \quad (14)$$

Since the quantities τ_r, $k_{\parallel}$ and $k_{\perp}$, $R_{\parallel}/R_{\perp}$ and η_b^0 and η_c^0 are known, the semi-minor axis length c can be computed readily by choosing an appropriate value of the parameter x.

Noting that the apparent hydrodynamic volume in the nematic state at 52 °C is quite close to that in THF at 35 °C (Fig. 6), we can estimate the value of x by assuming that the true hydrodynamic volumes are identical, viz. $(4\pi/3)ac^2 = (4\pi/3)R_{\parallel}R_{\perp}^2/x^3 = (4\pi/3)R_{h,iso}^3$. The resulting values of x, a, and c, together with the corresponding values of $R_{\parallel}$ and $R_{\perp}$, as well as the effective hydrodynamic radii, $R_{h\parallel}$ and $R_{h\perp}$, computed by fits to the data are listed in Table 5. We find that the mean value of x is 1.2, corresponding to a ratio $R_{nem}/R_{h,nem} = (R_{\parallel}^2 + 2R_{\perp}^2)^{1/2}/(ac^2)^{1/3} \sim 2.0$, which is substantially smaller than the equivalent ratio for a non-draining Gaussian coil $R_{iso}/R_{h,iso} \sim 3.0$. In fact, this result is not unreasonable, in view of the comb-like architecture of the SCLCP. We also remark that, as expected for a weakly prolate ellipsoid, $R_{h\parallel}$ is slightly smaller than $R_{h\perp}$ (Table 5, columns 8 and 9). A further result of interest is the different molecular weight dependence of the resulting values of $R_{\parallel}$ and $R_{\perp}$, which is displayed in the log–log plot shown in Fig. 7. A least-squares fit indicates that $R_{\parallel} \sim M_w^{0.50\pm0.06}$ and $R_{\perp} \sim M_w^{0.64\pm0.02}$. Assuming the stated value of $x = 1.2$ also applies at other temperatures (23 and 32 °C) in the nematic state, we extract values of $R_{\parallel}$ and $R_{\perp}$, which are plotted in Fig. 7. The results indicate a trend of increasing values of these size parameters with decrease in temperature, presumed to reflect an increase in rigidity of the chain backbone with increase in the nematic order parameter.

Concerning the different molecular weight dependences of $R_{\parallel}$ and $R_{\perp}$, evident in Fig. 7, we note that a similar phenomenon was previously observed in a SANS study of a polymethacrylate SCLCP in the nematic melt by Cotton et al. [12]. In that case, the chain conformation was determined to be oblate ($R_{\parallel} < R_{\perp}$) with $R_{\parallel} \sim M_w^{0.63\pm0.05}$ and $R_{\perp} \sim M_w^{0.48\pm0.03}$. The origin of this effect is unclear. However, as suggested by Cotton [12], it may reflect the crossover from wormlike to random conformational

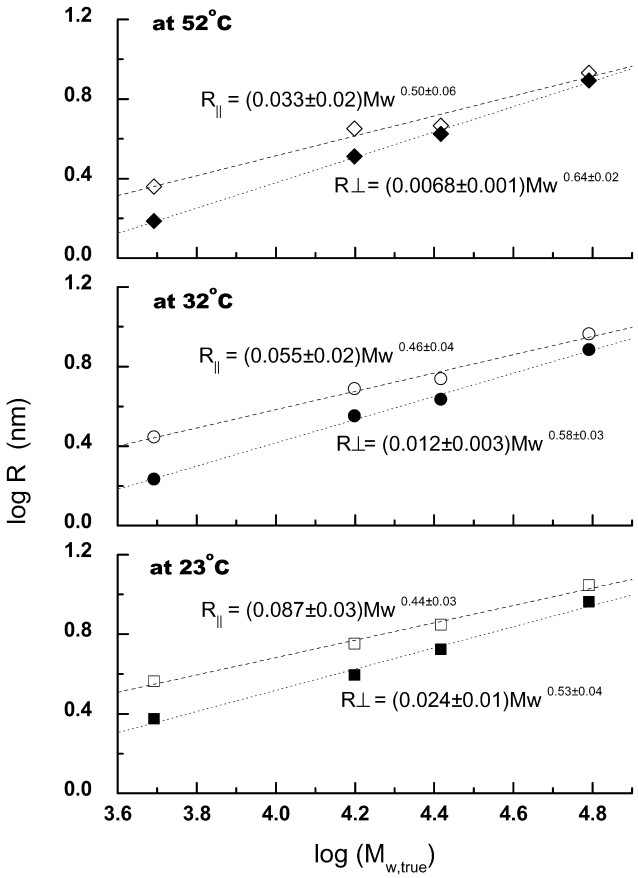

Fig. 7. Log–log plot of molecular weight dependence of anisotropic chain conformational dimensions, i.e. rms end-to-end distances $R_{\parallel}$ and $R_{\perp}$ for polyacrylate SCLCP in E48 at various temperatures derived via Eq. (14) with fitting parameter $x = 1.2$.

statistics coupled to the fact that the chain conformation is more confined in one direction relative to the nematic director. A similar analysis to the above cannot be carried out for the more polydisperse polysiloxane SCLCP. However, it is clear that dissimilar molecular weight scaling of $R_{\|}$ and $R_{\perp}$ is present also for the polysiloxane SCLCP, since as seen in Table 4, the ratio $R_{\|}/R_{\perp}$ decreases with increase in molecular weight.

4. Conclusion

We have investigated the ER behavior of dilute nematic solutions of an end-on SCLCP, having a polyacrylate backbone, and compared the results with an earlier study of a similar polymer, having the same spacer, but a polysiloxane backbone and a different mesogen. We find a common characteristic in that the molecular weight dependence of $\delta\eta_{on}$ is weak while that of $\delta\eta_{off}$ is strong. However, the numerical values of the molecular weight scaling exponents for the two polymers are different, being in each case significantly larger for the polyacrylate SCLCP. Application of the Brochard hydrodynamic theory indicates that for each polymer, the conformation is prolate ($R_{\|} > R_{\perp}$), and becomes more spherical with increase in molecular weight. The molecular weight dependence of the conformational relaxation time τ_r is also stronger for the polyacrylate SCLCP. Strikingly, for each SCLCP, the molecular weight scaling exponent of τ_r is essentially identical to that of the GPC hydrodynamic volume, V_h, in the isotropic solvent, THF.

These results indicate that the conformation of the polysiloxane SCLCP is more compact than the polyacrylate SCLCP, and that in each case, the molecular weight scaling of the hydrodynamic volume is only weakly affected by the nematic interaction. Microscopic analysis of the coil hydrodynamics within the Brochard model, assuming that the frictional coefficient parallel to the director is determined by the solvent Miesowicz viscosity η_b^0, while that perpendicular to the director is controlled by η_c^0, leads to intuitively reasonable values for the ratio of static to dynamic lengths.

Acknowledgments

A.M.J. acknowledges the National Science Foundation (DMR-0080114) and C.P. acknowledges the National Science Foundation (DMR-9806247) and the Ohio Board of Regents for financial support.

References

[1] Carlsson T, Skarp K. Mol Cryst Liq Cryst 1981;78:157.
[2] Skarp K, Carlsson T, Lagerwall ST. Mol Cryst Liq Cryst 1981;66:199.
[3] Yang IK, Shine AD. J Rheol 1992;36:1079.
[4] Yang IK, Shine AD. Macromolecules 1993;26:1529.
[5] Chiang YC, Jamieson AM, Kawasumi M, Percec V. Macromolecules 1997;30:1992.
[6] Chiang YC, Jamieson AM, Campbell S, Lin Y, O'Sidocky N, Chein LC, Kawasumi M, Percec V. Rheol Acta 1997;36:505.
[7] Yao N, Jamieson AM. Macromolecules 1997;30:5822.
[8] Carri GA, Muthukumar M. J Chem Phys 1998;109:11117.
[9] Brochard F. J Polym Sci, Polym Phys Ed 1979;17:1367.
[10] Yao N, Jamieson AM. Macromolecules 1998;31:5399.
[11] Cotton JP, Hardouin F. Prog Polym Sci 1997;22:795.
[12] Fourmaux-Demange V, Boué F, Brûlet A, Keller P, Cotton JP. Macromolecules 1998;31:801.
[13] Wang SQ. Macromolecules 1991;24:938.
[14] Kasko AM, Heintz AM, Pugh C. Macromolecules 1998;31:256.
[15] Kasko AM, Pugh C. Manuscript in preparation; 2002.
[16] Appelt B, Meyerhoff G. Macromolecules 1979;12:968.
[17] Happel J, Brenner H. Low Reynolds number hydrodynamics with special applications to particulate media. Englewood Cliffs, NJ: Prentice-Hall; 1983. p. 220–25.